

## **Synthesis of a forest of double/triple walled CNTs of uniform diameters by plasma enhanced CVD using mono-disperse iron oxide nanoparticles**

Ankur Baliyan<sup>1</sup>, Takashi Uchida<sup>2</sup>, Takahiro Fukuda<sup>2</sup>, Yoshikata Nakajima<sup>2</sup>,  
Tatsuro Hanajiri<sup>1,2</sup> and Toru Maekawa<sup>1,2,\*</sup>

<sup>1</sup> Graduate School of Interdisciplinary New Science, Toyo University, 2100, Kujirai,  
Kawagoe, Saitama 350-8585, Japan

<sup>2</sup> Bio-Nano Electronics Research Centre, Toyo University, 2100, Kujirai, Kawagoe,  
Saitama 350-8585, Japan

\* Corresponding author, e-mail: Maekawa@toyo.jp

---

### **Table of Contents**

1. Fe<sub>2</sub>O<sub>3</sub> nanoparticles at higher magnifications
2. Distribution of the diameter of Fe<sub>2</sub>O<sub>3</sub> nanoparticles
3. Morphologies of CNTs after manipulations
  - 3.1 Blocks of grown CNTs
  - 3.2 Folding of grown CNTs
4. Distribution of the internal diameter of grown CNTs
5. XPS analysis of nanoparticles
6. Detailed analysis of Raman spectra

### 1. Fe<sub>2</sub>O<sub>3</sub> nanoparticles at higher magnifications

The lattice fringes within the particles indicate that the particles are single crystal. The lattice spacing in the nanoparticles was exactly the same as that in bulk Fe<sub>2</sub>O<sub>3</sub>.

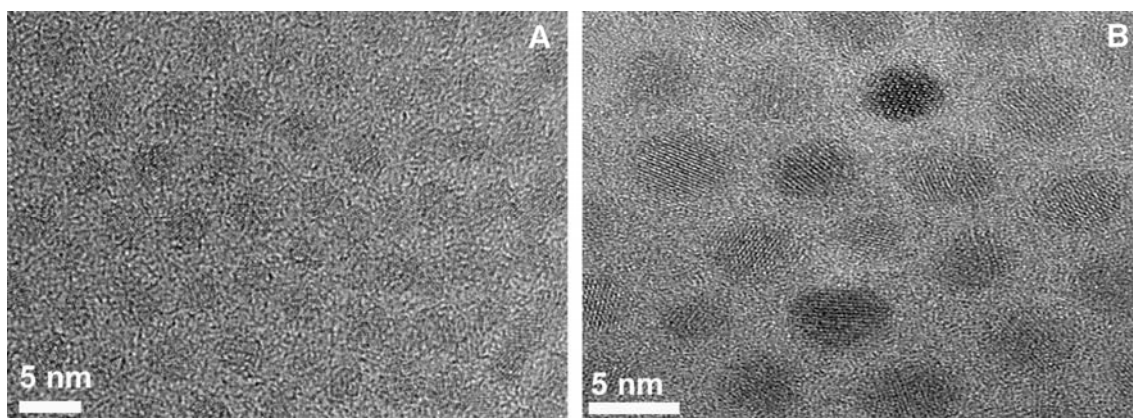


Figure S1 Crystalline structure of Fe<sub>2</sub>O<sub>3</sub> nanoparticles. (A) Particles of 3.8 nm in average diameter; (B) Particles of 4.5 nm in average diameter.

## 2. Distribution of the diameter of Fe<sub>2</sub>O<sub>3</sub> nanoparticles

The distribution of the diameter of Fe<sub>2</sub>O<sub>3</sub> nanoparticles is shown in Figure S2. The average diameter of nanoparticles was  $3.8 \pm 0.17$  nm (see Figure S2A) and  $4.5 \pm 0.43$  nm (Figure S2B).

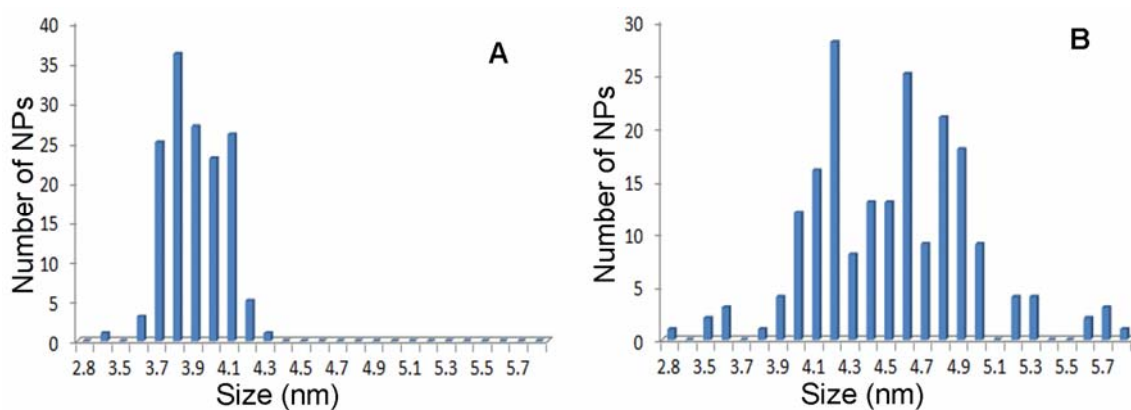


Figure S2 Distribution of the diameter of Fe<sub>2</sub>O<sub>3</sub> nanoparticles. (A) Particles of 3.8 nm in average diameter; (B) Particles of 4.5 nm in average diameter.

### 3. Morphologies of CNTs after manipulations

#### 3.1 Blocks of grown CNTs

The forest of CNTs was not fragmented into blocks during the growth process but the formation of blocks was caused by manhandling for SEM observations.

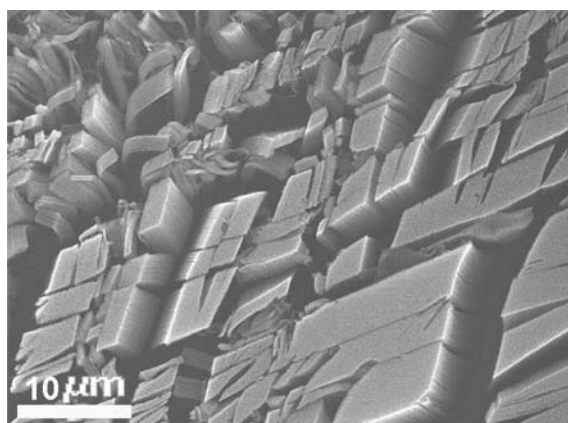


Figure S3 SEM image of blocks of grown CNTs.

### 3.2 Folding of grown CNTs

Vertically aligned carbon nanotubes (VA-CNTs) had weak interactions with the silicon substrate. When VA-CNTs were pulled with tweezers, the top layers of nanoparticles and a forest of VA-CNTs underneath were folded together, but the alignment of CNTs was still maintained. Therefore, the grown CNTs can be transferred to a desired substrate without losing their alignment.

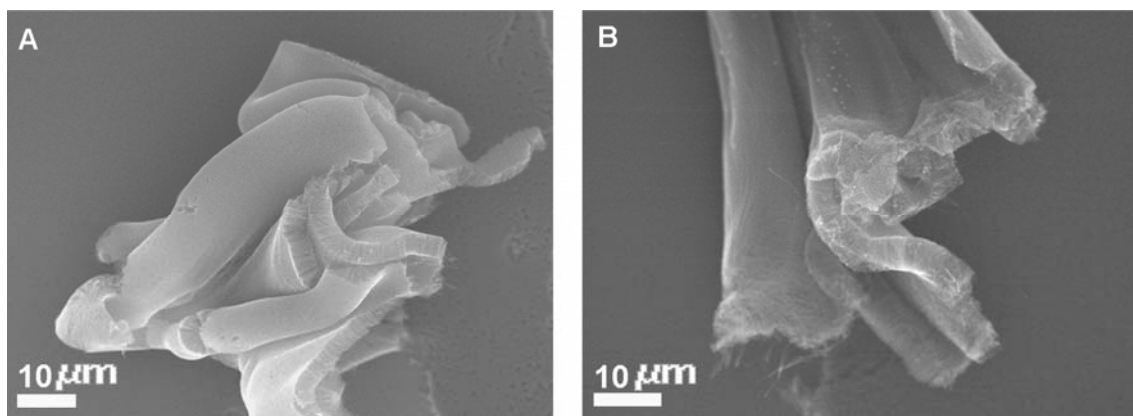


Figure S4 SEM images of folded sheets of grown CNTs after a manipulation with tweezers. (A) CNTs of 3.6 nm in average internal diameter; (B) CNTs of 4.2 nm in average internal diameter.

#### 4. Distribution of the internal diameter of grown CNTs

The distribution of the internal diameter of CNTs is shown in Figure S5. The average internal diameter of CNTs grown using nanoparticles of 3.8 nm in diameter was  $3.6 \pm 0.29$  nm (see Figure S5A), while that of CNTs grown using nanoparticles of 4.5 nm in diameter was  $4.2 \pm 0.32$  nm (Figure S5B).

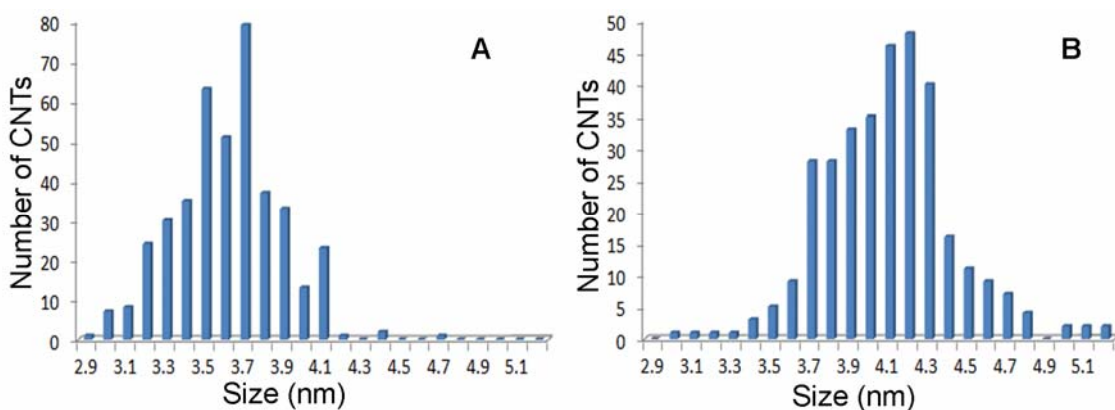


Figure S5 Distribution of the internal diameter of CNTs. (A) CNTs grown using particles of 3.8 nm in average diameter; (B) CNTs grown using particles of 4.5 nm in average diameter.

## 5. XPS analysis of nanoparticles

It is well known that iron oxide is reduced to iron at elevated temperature and in the presence of  $H_2$ . In the present study, the activity of catalytic nanoparticles was enhanced thanks to the reduction of iron oxide nanoparticles to metallic ones. We carried out X-ray photoelectron spectroscopy (XPS) analysis of nanoparticles to confirm the reduction of iron oxide nanoparticles to metallic ones, focusing on the Fe  $2p_{1/2}$  and Fe  $2p_{3/2}$  peaks, which is shown in Figure S6. The shift of the Fe  $2p_{1/2}$  and Fe  $2p_{3/2}$  peaks and the change in the gap between the binding energies corresponding to Fe  $2p_{1/2}$  and Fe  $2p_{3/2}$  peaks [1] tell that the catalytic iron oxide nanoparticles were reduced to metallic iron nanoparticles after the application of plasma and the raise in the temperature. Note that the Fe  $2p_{3/2}$  peak corresponding to  $Fe_2O_3$  still exists in the spectrum (see the red curve in Figure S6) even after reduction due to quick intrinsic oxidation nature of pure iron.

1. C.D. Wagner, W.M. Riggs, L.E. Davis, J.F. Moulder and G.E. Mullenberg, *Handbook of X-ray Photoelectron Spectroscopy*, 1979, page 76, (Perkin-Elmer Corp., Eden Prairie, MN, USA).

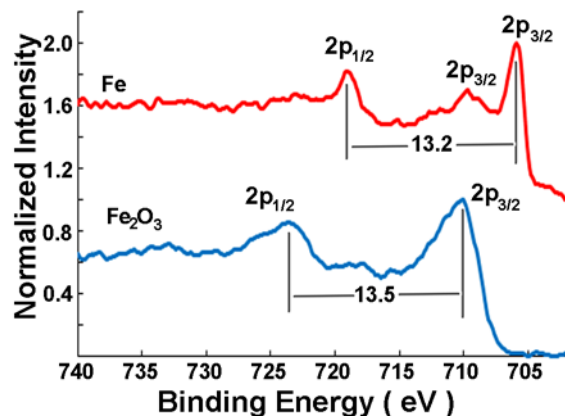


Figure S6 XPS of nanoparticles as an initial catalyst (blue curve) and after reduction with plasma (red curve).

## 6. Detailed analysis of Raman spectra

Raman spectra of CNTs with 633 and 325 nm excitation wavelengths are, respectively, shown in Figures 5A and 5B in the main text. The average diameters of CNTs were 3.6 and 4.2 nm. The G band represents the amount of graphitisation, while the D band the amount of defects associated with the carbon nanotubes. The radial breathing mode (RBM) can be seen between 188 and 278  $\text{cm}^{-1}$  when the excitation wavelength was 633 nm (see Figure 5A), which indicates that SWCNTs of smaller than 2 nm in diameter might have been produced [1]. However, no SWCNT of smaller than 2 nm in diameter was observed by TEM. Furthermore, the absence of the G band splitting into  $G^+$  and  $G^-$  also indicates that there are few SWCNTs produced [2]. It is therefore supposed that the RBM peaks might have come from a trace of SWCNTs of small diameters.

It is known that high G/D ratios are attributed to the presence of SWCNTs and low number density of defects in MWCNTs. In the present case, the G/D ratio was, respectively, 5.92 and 3.76 for CNTs of 3.6 and 4.2 nm in internal diameter when the excitation wavelength was 633 nm, whereas the ratio was 5.46 and 2.72 when the excitation wavelength was 325 nm. Note that the G/D ratio decreases with an ultraviolet excitation compared to that with a near-infrared excitation and that the ratio also decreases with an increase in the diameter of CNTs. It is therefore supposed that such high G/D ratios are attributed to high quality double/triple walled CNTs produced by the PECVD method since few SWCNTs of smaller than 2 nm in diameter were produced in the present case.

## References

1. N.T. Alvarez, F. Li, C.L. Pint, J.T. Mayo, E.Z. Fisher, J.M. Tour, V.L. Colvin and R.H. Hauge, *Chem. Mat.*, 2011, **23**, 3466.
2. M.S. Dresselhaus, G. Dresselhaus, R. Saito and A. Jorio, *Phys. Rep.-Rev. Sec. Phys. Lett.*, 2005, **409**, 47.